Cross sections of the ^{148}Sm(n,α)^{145}Nd reaction in the 4.8–5.3 MeV neutron energy range*

I. Chuprakov[1,2] E. Sansarbayar[2,3†] Guohui Zhang (张国辉)[4] Yu.M. Gledenov[2] G.Khuukhenkhuu [3] L. Krupa[5,6,7] Jie Liu (刘杰)[4] Haofan Bai (白浩帆)[4] Cong Xia (夏聪)[4] Zepeng Wu (邬泽鹏)[4,8] Wenkai Ren (任文凯)[4] D. Berikov[1,2] G. Ahmadov[2,9] A.K. Bekbayev[1,2,10] B. Mukhametuly[1,2,10] E.S. Korshikov[10] Y. Arynbek[1,2,10] O. Daulbayev[1,2]

[1]The Institute of Nuclear Physics, Ministry of Energy of the Republic of Kazakhstan, Almaty 050032, Kazakhstan
[2]Frank Laboratory of Neutron Physics, Joint Institute for Nuclear Research, Dubna 141980, Russia
[3]Nuclear Research Center, National University of Mongolia, Ulaanbaatar 210646, Mongolia
[4]State Key Laboratory of Nuclear Physics and Technology, Institute of Heavy Ion Physics, School of Physics, Peking University, Beijing 100871, China
[5]Flerov Laboratory of Nuclear Reactions, Joint Institute for Nuclear Research, Dubna 141980, Russia
[6]Institute of Experimental and Applied Physics, Czech Technical University in Prague, Husova 240/5, Prague 1, 110 00, Czech Republic
[7]Faculty of Science, Palacký University Olomouc, 17. listopadu 1192/12, 779 00 Olomouc, Czech Republic
[8]National Key Laboratory of Intense Pulsed Radiation Simulation and Effect, Northwest Institute of Nuclear Technology, Xi'an 710024, China
[9]Innovation and Digital Development Agency Nuclear Research Department, Gobu str. 20th km of Baku–Shamakhi Highway, AZ0100, Baku, Azerbaijan
[10]Al–Farabi Kazakh National University (IETP), 050040, Almaty, Kazakhstan

Abstract: The cross sections of the ^{148}Sm(n,α)^{145}Nd reaction were measured for the first time at neutron energies ranging from 4.8 to 5.3 MeV. The experiment was carried out on the Van de Graaff accelerator EG–5 at the Frank Laboratory of Neutron Physics, Joint Institute for Nuclear Research. Fast neutrons were produced via the ^{2}H(d,n)^{3}He reaction with a deuterium gas target. A twin gridded ionization chamber was used as the charged particle detector, with back–to–back ^{148}Sm samples mounted on tantalum backings at the common cathode. The absolute neutron flux was measured using the $^{238}U_3O_8$ sample. The obtained cross section data were compared with those from existing nuclear data libraries and theoretical calculations using the TALYS–1.96 code. The present results for the ^{148}Sm(n,α)^{145}Nd reaction are expected to resolve discrepancies among various nuclear evaluation data.

Keywords: nuclear reaction, ^{148}Sm, fast neutron induced reaction, fast neutrons, (n,α) reaction

DOI: 10.1088/1674-1137/add09a **CSTR:** 32044.14.ChinesePhysicsC.49074007

I. INTRODUCTION

Cross section data for charged particle emission reactions induced by fast neutrons are important in basic nuclear physics [1–5], nuclear astrophysics [6–8], and nuclear engineering [9]. Samarium isotopes are relatively high–yield fission products in nuclear reactors, making the accurate knowledge of their neutron cross sections essential for nuclear technology applications. The (n,α) reactions, in particular, are gas–producing and exothermic. The helium gas accumulated in the material causes [10] serious embrittlement problems.

Natural samarium is composed of five stable isotopes: ^{144}Sm, ^{149}Sm, ^{150}Sm, ^{152}Sm, and ^{154}Sm, together with two extremely long–lived radioisotopes, ^{147}Sm (half–life 1.06×10^{11} years) and ^{148}Sm (7×10^{15} years with abundance 11.24%).

Previously, we measured the (n,α) reaction cross-sections in the MeV energy region for the isotopes of ^{144}Sm, ^{147}Sm, and ^{149}Sm [11–16].

Currently, there are no cross section data for the ^{148}Sm(n,α)^{145}Nd reaction in the MeV neutron energy range. Existing evaluations in nuclear data libraries, such as ENDF/B–VIII.0 [17], ENDF/B–VII.1 [18], ENDF/B–VIII.1 [19], and JEFF–3.3 [20], provide identical evaluation results, while JENDL–5.0 [21] and ROSFOND–2010 [22] present different values. The ROSFOND–2010 evaluation differs from the latest version of the ENDF library, showing a discrepancy of approximately 1.5 times in our investigated neutron energy region.

In this paper, we present the first experimental measurements of the cross section for the ^{148}Sm(n,α)^{145}Nd re-

Received 31 January 2025; Accepted 24 April 2025; Published online 25 April 2025

* Supported by the Committee of Science of the Ministry of Science and Higher Education of the Republic of Kazakhstan (BR21881930)

† E-mail: sansar@nf.jinr.ru

©2025 Chinese Physical Society and the Institute of High Energy Physics of the Chinese Academy of Sciences and the Institute of Modern Physics of the Chinese Academy of Sciences and IOP Publishing Ltd. All rights, including for text and data mining, AI training, and similar technologies, are reserved.

action in the 4.8–5.3 MeV neutron energy range. Our measurements aim to resolve existing inconsistencies between various evaluated cross section data libraries. Additionally, we compare the experimental results with theoretical calculations using the TALYS–1.96 [23] code. By providing reliable cros-section measurements for the ^{148}Sm(n,α)^{145}Nd reaction, this work contributes to more accurate nuclear evaluations, enhancing our understanding of nuclear energy technology, nuclear physics, and stellar nucleosynthesis.

II. DETAILS OF EXPERIMENTS

The experiment was conducted at the EG–5 Van de Graaff accelerator at the Frank Laboratory of Neutron Physics, Joint Institute for Nuclear Research. The experimental setup, shown in Fig. 1, consisted of three main components: a mono–energetic neutron source, a twin gridded ionization chamber (GIC) as the charged particle detector, and a ^{3}He counter for monitoring the neutron flux.

A. Neutron source

Fast neutrons were generated via the ^{2}H(d,n)^{3}He reaction using a deuterium gas target. The gas cylinder vessel, which was 2 cm in length and 0.9 cm in diameter, was separated from the accelerator's vacuum tube by a 6.0 μm thick molybdenum foil. The pressure of the deuterium gas was 2.5 atm, and the incident deuteron beam current was approximately 2.5 μA. The energy range of the incident deuterons was 2.4–2.8 MeV to generate neutrons with energy 4.8 – 5.3 MeV.

B. Charged particle detector, data acquisition system and samples

The GIC with a common cathode was used as a charged particle detector. The structure of the GIC and its characteristics were presented in Ref. [11]. For the measurement of the ^{148}Sm(n, α)^{145}Nd reaction, a mixture of argon plus 3.0% carbon dioxide was employed as the working gas at a pressure of 3.0 atm. This allowed for the alpha particles to be stopped before reaching the grids. The grid electrodes were grounded, while the anode had a high voltage of +1800 V, and the cathode was at –2700 V. The cathode and anodes were covered with tantalum foil to reduce neutron induced background.

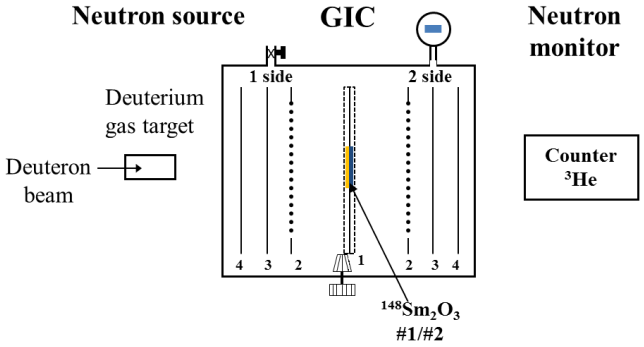

Fig. 1. (color online) Scheme of the experimental setup. 1, 2, 3, 4 – common cathode with samples, grids, anodes and shields of the GIC, respectively.

The detector signals were recorded using a 14 bit Pixie–16 module, with a sampling frequency of 250 MHz. The Pixie system consisted of a chassis (PXI6023–XIA 14, Wiener), an embedded controller (NI PXI–8820), and a high–speed digitizer (Pixie–16).

A sample changer with five sample positions was installed at the common cathode of the GIC, allowing the samples to be changed without opening the chamber [24]. Two $^{148}SmO_2$ samples and one $^{238}U_3O_8$ sample were prepared. All samples were deposited on tantalum backings with diamaters of 48 mm and thickness of 0.10 mm. The content of Sm isotopes in the samples are as follows: ^{144}Sm (0.04%), ^{147}Sm (2.05%), ^{148}Sm (91.20%), ^{149}Sm (5.27%), ^{150}Sm (0.55%), ^{152}Sm (0.60%), and ^{154}Sm (0.29%). The characteristics of the two $^{148}SmO_2$ samples and the $^{238}U_3O_8$ sample (for neutron flux measurement) are given in Table 1.

C. Neutron flux measurement and monitor

The absolute neutron flux was determined by detecting fission fragments from a $^{238}U_3O_8$ sample, which was positioned in one of the five sample positions at the GIC's common cathode. Additionally, a ^{3}He long counter at 0º with respect to the deuteron beam line was employed as a neutron flux monitor.

D. Simulation of measurements of the ^{148}Sm(n, α)^{145}Nd reaction

Before performing measurements, simulations were conducted to predict the experimental spectra of the ^{148}Sm(n,α)^{145}Nd reaction and potential interference reactions from other samarium isotopes, such as ^{147}Sm and ^{149}Sm, including (n,α) reactions involving the working gas. These simulations were carried out using Matlab software and TALYS–1.96 code. Cross sections, as well as angular and energy distributions from TALYS–1.96, were used as inputs for the calculations. Simulations were performed using a solid sample of samarium with a thickness of 2.94 mg/cm², and a mixture of argon with 3.0%

Table 1. Characteristics of samples.

Sample	Abundance (%)	Thickness/(mg/cm^2)	Diameter/mm
$^{148}SmO_2$ 01	91.20	2.94±0.04[a]	44.0
$^{148}SmO_2$ 02	91.20	3.10±0.03[a]	44.0
$^{238}U_3O_8$	99.999	0.475	44.0

a) Thickness of samarium only;

carbon dioxide was used as the working gas at a pressure of 3.0 atm. The calculations covered the neutron energy range from 4.8 to 5.3 MeV and determined the expected positions of events for the studied reaction, as well as background reactions that can mask the effect. Figure 2 shows the calculated two–dimensional cathode–anode spectra of alpha particles from the ^{148}Sm(n,α)^{145}Nd reaction at 5.3 MeV neutron energy emitted from a samarium sample in the forward and backward directions. The results quantitative assessment showed that the interference from ^{147}Sm(n,α) and ^{149}Sm(n,α) reactions is negligible (less than 3%).

III. MEASUREMENTS OF THE ^{148}Sm(n, a)^{145}Nd REACTION WITH FAST NEUTRONS.

A. Experimental procedure

Measurements for the ^{148}Sm(n,α)^{145}Nd reaction were carried out at neutron energies of 4.8, 5.1, and 5.3 MeV. The experimental procedure was performed in several steps at each energy point, as outlined below:

1. Calibration

The system was first calibrated using an alpha source to ensure accurate detector readings before starting the measurements.

2. Foreground measurements

Back–to–back ^{148}Sm samples were placed at the common cathode of the GIC to accurately measure the (n,α) reaction.

3. Neutron flux measurements

The absolute neutron flux was measured for each neutron energy point in a separate measurement using the ^{238}U(n,f) reaction. The $^{238}U_3O_8$ sample with the same dimension placed at the same sample position as the ^{148}Sm samples. The total fission counts from the $^{238}U_3O_8$ sample were used to determine the absolute neutron flux.

Figure 3 shows an example of the anode spectrum of the fission fragments from the ^{238}U(n,f) reaction, which was used to measure the absolute neutron flux.

The measurement durations were about 2 h for each neutron energy point.

4. Background Measurements

Background data were recorded using pure tantalum backings under the same experimental conditions as the foreground measurements. These background measurements were performed at the neutron energy point.

5. Recalibration

After each measurement, the system was recalibrated with the alpha source.

The ^{3}He long counter was used as a neutron flux monitor, positioned 3 m from the neutron source during all measurements at each energy point. The counts from the ^{3}He counter were used as a normalization factor in the cross section calculation.

The measurement durations for the foreground measurements were 36, 60, and 36 h at 5.3, 5.1, and 4.8 MeV, respectively. For the background measurements, the durations were 19, 39, and 19 h at the corresponding energy points. For the absolute neutron flux measurements, the duration is approximately 2 h for each energy point. The detection efficiencies for both fission and alpha events were calculated using Monte Carlo simulations. The detection efficiency is defined as the ratio of counts within the threshold range to the total counts in the simulated spectrum. The details of the simulations are described in Ref. [25]. The detection efficiencies for fission fragments (ε_f) and alpha particles (ε_α) were determined to be 86% and 87%, respectively. These values were used to correct for efficiencies in the cross section calculation.

After data collection, the cathode–anode two–dimensional spectra were analyzed for both foreground and background measurements. Figures 4 and 5 shows the

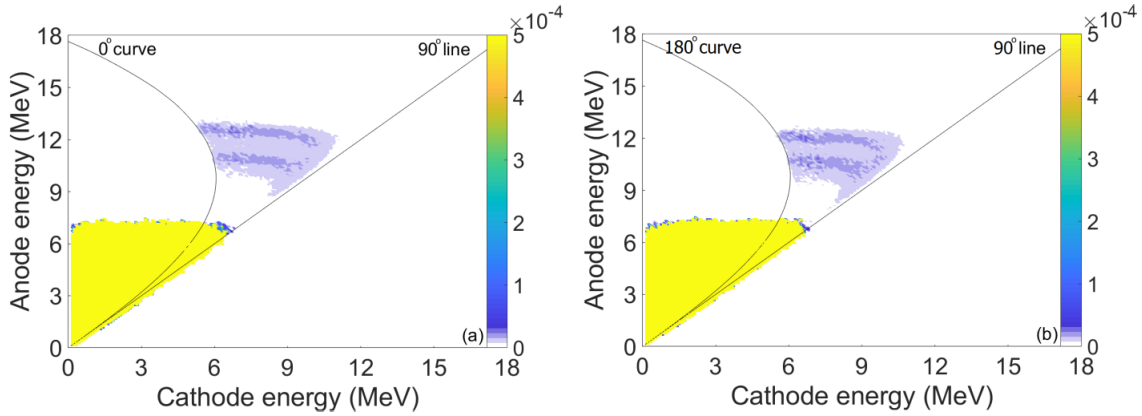

Fig. 2. (color online) Calculated two–dimensional cathode–anode spectra of alpha particles from the ^{148}Sm(n,α)^{145}Nd reaction at 5.3 MeV neutron energy: (a) forward and (b) backward directions.

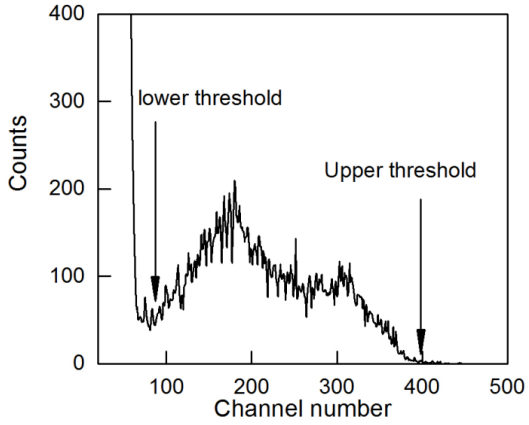

Fig. 3. The cathode spectrum of fission fragments for measuring the absolute neutron flux of the ^{238}U(n,f) reaction at 5.3 MeV neutron energies.

two–dimensional foreground (a) and background (b) spectra of the ^{148}Sm(n,α)^{145}Nd reaction at 5.3 MeV neutron energy in the forward and backward direction, respectively. Figure 6 presents the anode projection spectrum after subtracting background events from foreground events. A selection cut is then applied based on simulation results, which predict the expected distribution of α events from the ^{148}Sm(n,α)^{145}Nd reaction. The selected area is used to generate the anode projection spectrum for further analysis. Additionally, background events are subtracted while accounting for differences in measurement durations, and the ^{3}He counter counts are used for normalization.

The cross section ($\sigma_{n,\alpha}$) for the ^{148}Sm(n,α)^{145}Nd reaction was determined using the following formula:

$$\sigma_{n,\alpha} = K \cdot \sigma_{n,f} \frac{N_\alpha}{N_f} \frac{\epsilon_f}{\epsilon_\alpha} \frac{N_{^{238}\mathrm{U}}}{N_{^{148}\mathrm{Sm}}}, \quad (1)$$

where K = He$_f$/He$_\alpha$, with He$_f$ and He$_\alpha$ representing the counts of the ^{3}He counter during the measurements of the ^{238}U(n,f) and ^{148}Sm(n,α)^{145}Nd reactions, respectively.

$\sigma_{n,f}$ is the cross section for the ^{238}U(n,f) reaction from the ENDF/B–VIII.0 library.

N_α and N_f refer to the number of alpha and fission

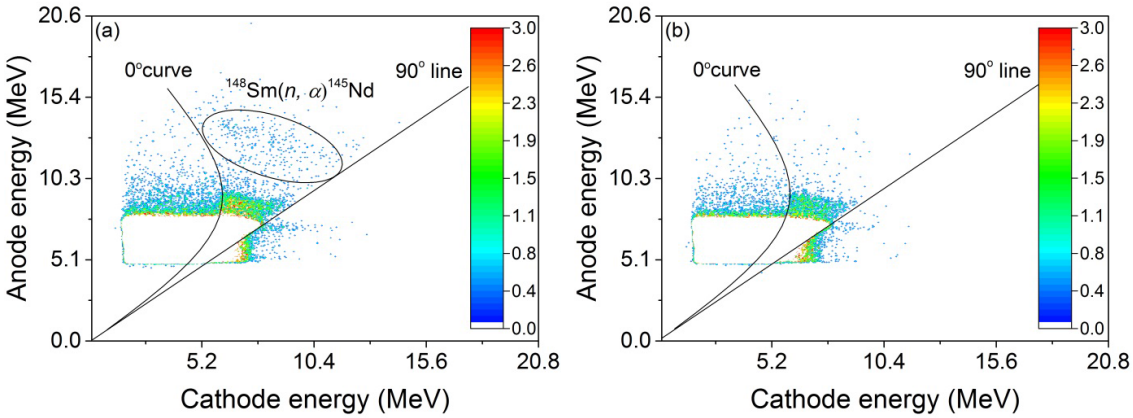

Fig. 4. (color online) Two–dimensional foreground (a) and background (b) spectra of the ^{148}Sm(n,α)^{145}Nd reaction in the forward direction at 5.3 MeV neutron energy.

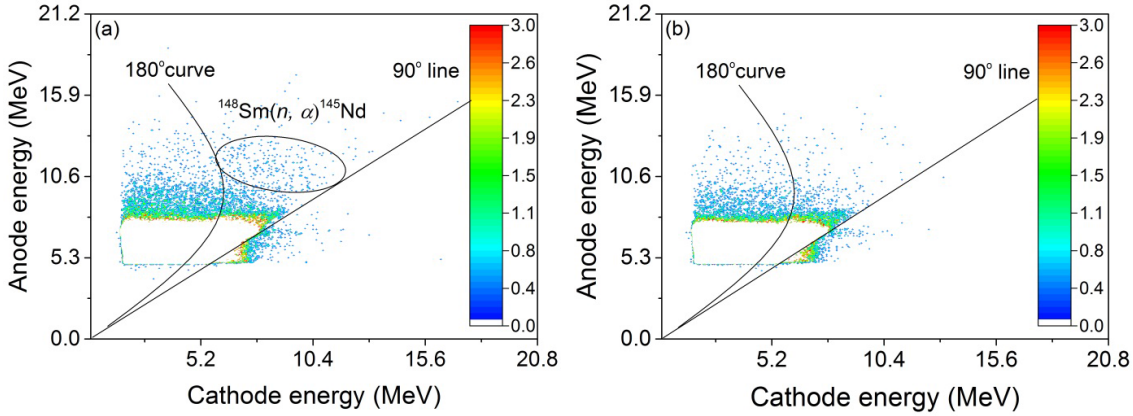

Fig. 5. (color online) Two–dimensional foreground (a) and background (b) spectra of the ^{148}Sm(n,α)^{145}Nd reaction in the backward direction at 5.3 MeV neutron energy.

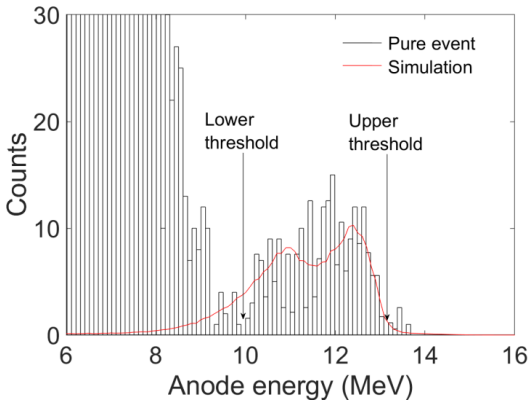

Fig. 6. (color online) The anode projection spectrum of the ^{148}Sm(n,α)^{145}Nd reaction in the forward direction at 5.3 MeV neutron energy.

events, respectively, values of which are determined after distinguishing background events within the specified energy thresholds for the reactions.

ε_f and ε_α are the detection efficiencies of the fission and alpha events.

N^{238}_{U} and N^{148}_{Sm} are the atom numbers in the ^{238}U and ^{148}Sm samples, respectively.

B. Results and discussions

The experimental cross sections for the ^{148}Sm(n, α)^{145}Nd reaction were obtained using Equation (1). The uncertainty was calculated using the error propagation formula. The primary source of uncertainty arises from the number of alpha events, which includes contributions from statistical errors and background subtraction, particularly influenced by the valid–event–area cut and the energy threshold cut. The sources of the uncertainty and their magnitudes are presented in Table 2. Consequenlty, the total uncertainty in the ^{148}Sm(n,α)^{145}Nd reaction cross sections ranges from 13% to 20%.

The measured cross section at each neutron energy was obtained by summing the forward and backward cross sections. Cross sections and forward/backward ratios in the laboratory reference system for ^{148}Sm(n,α)^{145}Nd reaction are given in Table 3. The ^{148}Sm(n,α)^{145}Nd reaction cross sections are shown in Fig. 7, which compared with the data from different evaluation libraries and TALYS–1.96 calculations using default and adjusted parameters as listed in Table 4.

We performed calculations using three sets of parameters in TALYS–1.96: default input parameters with the Avrigeanu [26] alpha–particle optical model potential (AOMP), default input parameters with the Atomki–V2 [27–29] AOMP, and adjusted parameters as listed in Table IV. The calculations using the default Avrigeanu AOMP significantly underestimated the experimental cross sections in the 4.8–5.3 MeV energy range. A slight improvement was observed when the Atomki–V2 AOMP was used with the default parameters. The calculated cross sections with Atomki–V2 AOMP were about 20% higher than those obtained with the Avrigeanu AOMP, but they still remained much lower than the experimental data. Given these results, we will provide a detailed theoretical analysis in a follow–up paper which will include all of our Sm(n, α) measurement data [11–16].

In the present work, TALYS–1.96 calculations using the adjusted OM parameters and the pairing shift for the Fermi gas level density (as listed in Table IV) give much better results, leading to significantly improved agreement across the measured energy range of 4.8–5.3 MeV.

Our measured cross sections are significantly lower than the evaluated values in ENDF/B–VIII.0, ENDF/B–VII.1, ENDF–VIII.1 and JEFF–3.3 libraries which are identical (by a factor of 1.2 to 1.4), in the neutron energy range of 4.8 to 5.3 MeV. Our experimental data are consistent with the ROSFOND–2010 evaluations at the two lower energy points and with the JENDL–5.0 library at 5.3 MeV neutron energy.

Table 2. Sources of the uncertainty.

Source	Magnitudes (%)
N^{238}_{U}	2.0
N^{148}_{Sm}	3.0
$\sigma_{n,f}$	0.7
N_α	12–18
N_f	3.0
σ_α	13 - 20
ε_f	2.0
ε_α	2.0

Table 3. Measured (n,α) cross section data and forward/backward ratios in the laboratory reference system for the ^{148}Sm(n,α)^{145}Nd reaction.

Energy,	Cross sections, mbarn			
/MeV	Forward	Backward	forward/backward ratio	Total
4.8	0.033±0.008	0.023±0.007	1.43	0.056±0.011
5.1	0.042±0.008	0.029±0.007	1.45	0.071±0.012
5.3	0.06±0.01	0.04±0.008	1.50	0.1±0.013

IV. CONCLUSIONS

The cross section for the ^{148}Sm(n,α)^{145}Nd reaction was systematically measured with high accuracy at neutron energies of 4.8, 5.1, and 5.3 MeV. These measurements represent the first experimental results in the MeV energy region. The experiments were performed on the EG–5 Van de Graaff accelerator using the GIC charged particle detector, enriched $^{148}SmO_2$ samples, and $^{238}U_3O_8$

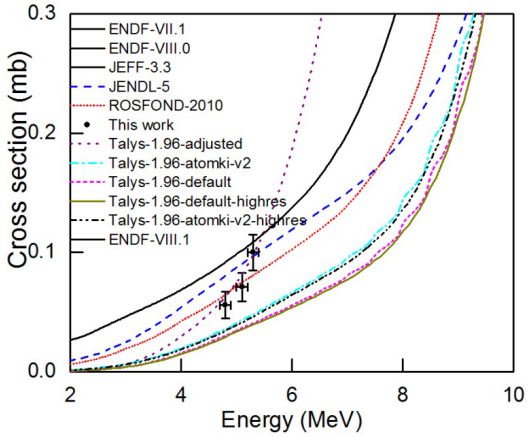

Fig. 7. (color online) Experimental and evaluated cross sections for the ^{148}Sm(n,α)^{145}Nd reaction compared with the calculated results from TALYS–1.96.

samples. The present experimental data are significantly lower than the values obtained in the ENDF/B–VIII.0, ENDF/B–VII.1, ENDF-VIII.1, and JEFF–3.3 libraries by a factor of 1.2 to 1.4. Our experimental data are consistent with the ROSFOND–2010 evaluations at the two lower energy points and with the JENDL–5.0 library at 5.3 MeV neutron energy, and the TALYS–1.96 calculations using the adjusted parameters produced results that were consistent with our experimental data across the 4.8 – 5.3 MeV neutron energy range.

Table 4. Adjusted input parameters of the TALYS–1.96.

Keyword	Parameters
ldmodel	2
Ldmodelcn	1
Alphaomp	6
Rvadjust	a 0.995
Avadjust	a 0.995
Aadjust	60 145 1.28
rvadjust	n 1.018 –0.2 0.2 0. 0.98
Pshiftadjust	62 148 0.60
Rvadjust	p 1.10
Avadjust	p 1.10
Gnadjust	62 149 0.94
Gpadjust	62 149 0.94

ACKNOWLEDGMENTS

The authors gratefully acknowledge the help from Dr. Peter Mohr for his invaluable assistance in calculating the cross sections using the TALYS code. We also extend our thanks to the operational team of the Van de Graaff accelerator EG–5 for their essential support and collaboration.

References

[1] V. N. Levkovsky, Yad. Fiz. **18**(4), 705 (1973)
[2] G. Khuukhenkhuu, Yu. M. Gledenov, M. V. Sedysheva *et al.*, Phys. Part. Nuclei Lett. **11**, 749 (2014)
[3] R. Chhetri, M. Sharma, J. Kaur *et al.*, J. Phys. : Conf. Ser. **2663**, 012059 (2023)
[4] D. J. Buss and R. K. Smither, Phys. Rev. C **2**, 1513 (1970)
[5] Yu. P. Popov, Nucl. Phys. A **188**, 212 (1972)
[6] R. Reifarth *et al.*, J. Phys. G: Nucl. Part. Phys. **41**, 053101 (2014)
[7] R. R. Winters *et al.*, Astrophys. J. **300**, 41 (1986)
[8] F. Käppeler, R. Gallino, S. Bisterzo *et al.*, Rev. Mod. Phys. **83**(1), 157 (2011)
[9] U. Kannan, Life Cycle Reliab Saf. Eng. **9**, 135 (2020)
[10] M. B. Chadwick, E. Dupont, E. Bauge *et al.*, Nuclear Data Sheets, **118**, 1 (2014).
[11] Yu. Gledenov, G. h. Zhang, G. Khuukhenkhuu*et al.*, EPJ Web of Conferences **146**, 11033 (2017)
[12] Y. M. Gledenov, G. Zhang, G. Khuukhenkhuu *et al.*, Phys. Rev. C, **82**(1), 014601 (2010)
[13] Y. M. Gledenov, P. E. Koehler, J. Andrzejewski *et al.*, Phys. Rev. C, **62**(4), 042801 (2000)
[14] Yu. M. Gledenov *et al.*, Phys. Rev. C, **80**(4), 044602 (2009)
[15] G. Zhang, Y. M. Gledenov, G. Khuukhenkhuu *et al.*, Phys. Rev. Lett. **107**(25), 252502 (2011)
[16] Yu. M. Gledenov, M. Sedysheva, G. Zhang *et al.* Journal of The Korean Physical Society **59**(2), 1693 (2011)
[17] M. B. Chadwick *et al.*, Nucl. Data Sheets, **112**(12), 2887 (2011)
[18] D. A. Brown *et al.*, Nucl. Data Sheets, **148**, 1 (2018)
[19] ENDF/B-VIII. 1, https://www.nndc.bnl.gov/endf-releases/?version=B-VIII.1
[20] A. J. M. Plompen, O. Cabellos, C. De Saint Jean *et al.*, Eur. Phys. J. A **56**, 181 (2020)
[21] O. Iwamoto, N. Iwamoto, S. Kunieda *et al.*, Journal of Nuclear Science and Technology, **60**(1), 1 (2023)
[22] S. V. Zabrodskaya, A. V. Ignatyuk, V. N. Koshcheev *et al.*, Vopr. At. Nauki Tekhn. Ser. Yad. Konst. **1**, 3 (2007)
[23] A. J. Koning, S. Hilaire, and S. Goriely, Eur. Phys. J. A **59**, 131 (2023)
[24] X. Zhang, Z. Chen, Y. Chen *et al.*, Phys. Rev. C **61**, 054607 (2000)
[25] H. y. Jiang *et al.*, Chin. Phys. C **44**, 114102 (2020)
[26] V. Avrigeanu, M. Avrigeanu, and C. Mănăilescu, Phys. Rev. C, **90**(4), 044612 (2014)
[27] P. Mohr, Zs. Fülöp, Gy. Gyürky *et al.*, Phys. Rev. Lett. **124**(25), 252701 (2020)
[28] P. Mohr, Zs. Fülöp, Gy. Gyürky *et al.*, At. Data Nucl. Data Tables **142**, 101453 (2021)
[29] P. Mohr, (2024, December), Private communication